Biogeosciences Discuss., 8, 4917–4952, 2011
www.biogeosciences-discuss.net/8/4917/2011/
doi:10.5194/bgd-8-4917-2011

Biogeosciences Discussions

Nitrogen uptake by phytoplankton in the Atlantic sector of the Southern Ocean during late austral summer

W. R. Joubert[1,2], **S. J. Thomalla**[1,2], **H. N. Waldron**[2], **and M. I. Lucas**[3]

[1]Council for Scientific and Industrial Research, P.O. Box 320, Stellenbosch, 7599, South Africa
[2]Department of Oceanography, University of Cape Town, Private Bag X3, 7701, South Africa
[3]Department of Zoology, University of Cape Town, Private Bag X3, 7701, South Africa

Received: 6 April 2011 – Accepted: 26 April 2011 – Published: 23 May 2011

Correspondence to: W. R. Joubert (wjoubert@csir.co.za)

Published by Copernicus Publications on behalf of the European Geosciences Union.

Abstract

As part of the Bonus-Good Hope (BGH) campaign, ^{15}N-labelled nitrate, ammonium and urea uptake measurements were made along the BGH transect from Cape Town to ~60° S in late austral summer, 2008. Our results are categorised according to distinct hydrographic regions defined by oceanic fronts and open ocean zones. Nitrogen uptake (ρN) in the oligotrophic Subtropical Zone (STZ) was dominated by ρ urea, which contributed up to 70 % of ρN. High regenerated ρN in the STZ resulted in low f-ratios ($f = 0.2$). Size fractionated chlorophyll data showed that the greatest contribution (>50 %) of picophytoplankton (<2 µm) were found in the STZ, consistent with a community based on regenerated production. The Subantarctic Zone (SAZ) showed the greatest total integrated ρN (10.3 mmol m^{-2} d^{-1}), mainly due to enhanced light and nutrient supply within an anticyclonic eddy observed in this region. A decrease in the contribution of smaller size classes to the phytoplankton community was observed with increasing latitude, concurrent with a decrease in the contribution of regenerated production. Higher f-ratios observed in the SAZ ($f = 0.49$), Polar Frontal Zone ($f = 0.41$) and Antarctic Zone ($f = 0.45$) relative to the STZ ($f = 0.2$), indicate a higher contribution of ρNO_3 relative to total ρN and potentially higher export production. Greater contribution of regenerated uptake to $\int\rho$N in the northern sector of the cruise resulted from increased ambient regenerated nutrient concentrations, shallow mixed layers in the north (~40 m) relative to the regions further south (~100 m). Higher $\rho\int$N rates also correspond with higher surface iron concentrations. No clear correlation was observed between carbon export estimates derived from new production and ^{234}Th flux. In addition, export derived from ^{15}N estimates were 2–20 times greater than those based on ^{234}Th flux. Variability in the magnitude of export is likely due to intrinsically different methods, compounded by differences in integration time scales for the two proxies of carbon export.

BGD
8, 4917–4952, 2011

1 Introduction

The Southern Ocean is considered one of the most important ocean sinks of atmospheric CO_2 (Caldeira and Duffy, 2000; Sigman and Boyle, 2000), making it important in understanding the global carbon cycle. Primary productivity in the Southern Ocean plays a key role in the biological uptake of atmospheric CO_2 (Metzl et al., 1999; Takahashi et al., 2002). Phytoplankton biomass typically shows low chlorophyll a (chl-*a*) ($< 0.5\,mg\,m^{-3}$) in open ocean waters of the Southern Ocean (Tréguer and Jacques, 1992; Banse, 1996; Moore and Abbott, 2000), while localised elevated chl-*a* ($> 1\,mg\,m^{-3}$; Moore and Abbott, 2000) are often associated with mesoscale upwelling at hydrographic fronts (Laubscher et al., 1993; Comiso et al., 1993; Moore and Abbott, 2002; Sokolov and Rintoul, 2007), the marginal ice zone (MIZ) (Smith and Nelson, 1986; Sedwick and DiTullio, 1997) and regions of shallow bathymetry around Subantarctic islands (Blain et al., 2001; Pollard et al., 2002; Korb and Whitehouse, 2004; Seeyave et al., 2007; Whitehouse et al., 2008). Under-utilization of available macronutrients by phytoplankton production results in the prevalent high nutrient low chl-*a* (HNLC) condition (Chrisholm and Morel, 1991) of the Southern Ocean. Despite a high inventory of available macronutrients, low chl-*a* concentrations are maintained by bottom-up controls of phytoplankton production through light, iron, and silicate limitation (Martin et al., 1990; Bathmann et al., 1997; Boyd et al., 2001, 2002, 2007; Moore and Abbott, 2002; Arrigo et al., 2008), as well as by top-down grazing control (Banse, 1991; Cullen, 1991; Price et al., 1994; Smetacek et al., 2004; Behrenfeld, 2010). These factors regulating primary production all modify carbon export and thus play a key role in determining the strength of the Southern Ocean biological carbon pump.

Measurements of phytoplankton production throughout the euphotic layer using ^{15}N stable isotopes (Dugdale and Goering, 1967) have often been used to infer carbon export into the ocean interior based on the *f*-ratio (Eppley and Peterson, 1979; Savoye et al., 2004). This approach to measuring carbon export relies on a number of underlying assumptions which include steady state conditions, no storage of nitrogen

BGD
8, 4917–4952, 2011

in surface waters (Eppley and Peterson, 1979), and minimal euphotic layer nitrification (Bianchi et al., 2007; Yool et al., 2007). In addition the use of stoichiometric ratios to convert nitrogen uptake (ρN) to carbon equivalents may be compromised by non-Redfield behaviour in the cellular response to available light, iron and nutrients (Brzezenski et al., 2003; Arrigo, 2005; Moore et al., 2007). Although nitrification in surface waters is particularly important in oligotrophic ocean regions, this process does not appear to be significant in nitrate replete environments (Yool et al., 2007; Lucas et al., 2007; Clark et al., 2008). Despite its limitations, the f-ratio therefore remains a useful proxy for estimating potentially "exportable production" (Sambrotto and Mace, 2000) in nutrient rich polar oceans.

Iron limited phytoplankton production in HNLC environments is now firmly established through a number of artificial (De Baar et al., 2005; Boyd et al., 2007) and natural iron fertilization experiments (Blain et al., 2001, 2007; Pollard et al., 2007). Iron is important in phytoplankton metabolism for processes such as nitrate reduction mediated by reductase enzymes (Morel et al., 1991), as well as in iron dependent photosynthetic redox reactions (Raven, 1988; Cochlan et al., 2008). Furthermore, co-limitation of iron and light influences phytoplankton processes (Raven, 1990; Boyd et al., 1999; Cochlan et al., 2002; Moore et al., 2007). Nitrate uptake is particularly sensitive to lower light compared to either ammonium or urea uptake, so that a decreased f-ratio with increasing depth can be expected concurrent with diminishing light, exacerbated by any iron stress (Glibert and Garside, 1992). Relief from iron stress favours faster rates of nitrate uptake, higher f-ratios and larger phytoplankton cells which can escape grazing pressure (Smetacek et al., 2004). Regenerated production on the other hand, has a lower light and iron demand, can frequently be satisfied by regenerated iron supply rather than new iron inputs (Bowie et al., 2001), and is typically characterised by smaller taxonomic groups.

This paper reports measurements of new and regenerated uptake rates and f-ratios (as a proxy for export) in surface waters of the Atlantic sector of the Southern Ocean in late austral summer 2008. The cruise formed part of the Bonus-GoodHope programme

BGD
8, 4917–4952, 2011

(BGH), which aims to understand large-scale inter-ocean basin exchanges and to characterise biogeochemical processes involved in trace element, nitrogen and carbon cycling. The cruise crossed a number of mesoscale features and major hydrographic fronts; namely the Subtropical Front (STF), the Sub-Antarctic Front (SAF), the Polar Front (PF), the Southern Antarctic Circumpolar Current Front (SAccF) and the Southern Boundary (Sbdy) (Fig. 1). Results from this study characterise ρN dynamics and f-ratios across different hydrographic regions and investigates their relation to MLD, light, macro-nutrient and dissolved surface iron concentrations. We compare our data with ^{15}N estimates of production in other areas of the Southern Ocean, as well as with ^{234}Th based estimates of carbon export measured during the BGH cruise.

2 Methods

2.1 Sampling and cruise track

The first sampling cruise (LEG 1) on board the R/V *Marion Dufresne* was conducted from 8 February–18 March 2008. The cruise transect (Fig. 1) started on the shelf outside Cape Town (South Africa) at the 200 m isobath and followed the GoodHope – A21 transect in a south-westerly direction to the 0° meridian, then continued south to 58° S. A total of 79 sampling stations were completed, 12 of which were targeted for ρN incubations using ^{15}N tracer techniques (Slawyk and Collos, 1977; Dugdale and Wilkerson, 1986).

2.2 Hydrography

Water mass characteristics of the section sampled were determined from temperature, salinity (and density) measured with a CTD (SEABIRD 911plus) mounted on a SEABIRD rosette.

BGD
8, 4917–4952, 2011

2.3 Nutrient analyses

Ambient concentrations of NH_4-N and urea-N were determined manually by the colorimetric method of Grasshoff et al. (1983), scaled to 5 ml samples. Ambient NO_3-N and $Si(OH)_4$-Si concentrations were analyzed on a Bran and Lubbe AAIII autoanalyser, as described in Tréguer and Lecorre (1975).

2.4 Chlorophyll-*a*

Total chl-*a* samples were collected in the upper 300 m at 6 depths from all CTD stations and 10 depths at all the ρN experiment stations. The samples were filtered onto 25 mm Whatman GF/F filters, extracted in 6 ml Acetone prior to fluorometric determination on a Turner Designs AU-10 fluorometer (Strickland and Parsons, 1972). Phaeopigments were determined by reading the fluorescence after acidification with 2–3 drops of 10 % hydrochloric acid. Size-fractionated chl-*a* determinations were collected opportunistically from surface water sampling. Size-fractionated chl-*a* concentrations were determined by screening samples through a 200 µm mesh (< 200 µm fraction), and a 20 µm mesh (< 20 µm fraction), followed by filtration onto Whatman GF/F filters. The < 2 µm fraction was obtained by filtering a sample through a 2 µm Nuclepore membrane filter and thereafter collecting the filtrate on a Whatman GF/F filter. Microphytoplankton (20–200 µm) were determined by subtracting the < 20 µm fraction from the < 200 µm fraction; nanophytoplankton (2–20 µm) by subtracting the < 2 µm fraction from the < 20 µm fraction, while picophytoplankton were represented by the < 2 µm fraction. Chl-*a* and phaeopigment concentrations of each fraction were determined as above.

2.5 POC and PON

Particulate organic carbon (POC) and nitrogen (PON) were determined by filtering 1 l samples onto pre-ashed 25 mm Whatman GF/F filters that were frozen at −20 °C until analysis ashore. Samples were then oven-dried at 45 °C, acid fumed with sulphuric

BGD
8, 4917–4952, 2011

acid to drive off inorganic carbon and pelletted into tin cups (8 × 5 mm) prior to analysis on a Thermo Finnegan Flash EA1112 elemental CHN analyser.

2.6 Nitrogen uptake measurements

To determine depth integrated nitrogen uptake ($\int \rho N$), samples were collected at 5 underwater irradiance levels (100 %, 50 %, 25 %, 10 % and 1 %) measured using an underwater PAR (400–700 nm) sensor attached to the CTD rosette. Three bulk samples (2 L each) from each light level were pre-screened through a 200 µm plankton mesh to exclude zooplankton grazers and transferred into borosilicate glass Schott bottles. Aliquots of 200 µl stock solutions of $K^{15}NO_3$ (1 µmol 100 µl^{-1}), $^{15}NH_4Cl$ (0.1 µmol 100 µl^{-1}) and $CO(^{15}NH_2)_2$ (0.1 µmol 100 µl^{-1})) were added, one to each of the three bottles from all light depths for ρN incubations. The ^{15}N enrichment was ~ 10 % for each nutrient, assuming an average ambient NO_3 concentration of 10 µmol l^{-1}, and 1 µmol l^{-1} for ammonium and urea. Incubation bottles were placed inside a perspex tank covered with neutral density filters to re-create the appropriate light environment. Temperature was maintained at sea surface temperature (SST) by circulating surface water through the incubation tanks. Samples were incubated for 24 h and terminated by filtration onto ashed 47 mm Whatman GF/F filters, which were then dried at 45 °C before later isotopic analyses.

2.7 Isotope analyses

Particulate matter collected on the Whatman GF/F filters were pelletted and placed 8 × 5 mm into tin capsules prior to isotopic analysis. Analyses were carried out on a Delta V Plus stable light isotope mass spectrometer interfaced to a Thermo Finnegan Flash EA1112 Elemental Analyser. Natural abundance for nitrogen was 0.3663 atom % ^{15}N. Values were scaled upwards to reflect the proportion of the sub-sampled area relative to the total filtered area. Sulphanilamide and urea were used as calibration standards for carbon and nitrogen determinations. Uptake rates for nitrogen were

BGD
8, 4917–4952, 2011

calculated as described by Dugdale and Wilkerson (1986), without correction for isotopic dilution in the case of NH_4 uptake.

3 Results

3.1 Hydrography

The BGH meridional cruise track crossed all the major hydrographic fronts and open ocean regions commonly recognised in the Southern Ocean (Orsi et al., 1996) (Fig. 1). The frontal positions during the cruise were determined using potential temperature criteria (Speich et al., 2011) (Fig. 2). The region north of the STF was defined as the Subtropical Zone (STZ) where SST exceeded 14 °C and salinity exceeded 35 psu (Fig. 2). The Sub-Antarctic zone (SAZ) lay between the STF (42.2° S) and the SAF (44.2° S), where SST fell in the range 9–14 °C, and surface salinity between 34–35 psu. In this zone, an intense anticyclonic eddy ("anticyclone M") of Indian Ocean origin was observed (at 42.9° S–44° S) over the Agulhas Ridge (Fig. 2). The Polar Front Zone (PFZ) extended from the SAF to the APF (Pollard et al., 2002) at 50.2° S, where SST decreased from 10–5 °C and surface salinity was < 34 psu (Fig. 2). The Antarctic Zone (AZ) was found south of the APF where temp was < 3 °C and salinity was ~ 34 psu. The following results are presented according to the four zones defined above (STZ, SAZ, PFZ and AZ).

3.2 Nutrients

In the STZ, surface nutrient concentrations (Fig. 3a, b) showed typical oligotrophic conditions, with surface NO_3 concentrations < 0.05 µmol l^{-1} (Fig. 3a), while surface $Si(OH)_4$ concentrations were typically < 2 µmol l^{-1} (Fig. 3b). Surface NH_4 concentrations were depleted (< 0.1 µmol l^{-1}), while urea concentrations were variable, ranging from 0.22–1.51 µmol l^{-1} (Table 1). In the SAZ, a gradual increase in surface NO_3 concentrations

BGD
8, 4917–4952, 2011

was observed ranging from 5–15 µmol l^{-1}, but reaching 20 µmol l^{-1} below 100 m depth (Fig. 3a, Table 1). $Si(OH)_4$ concentrations were depleted (< 1 µmol l^{-1}) throughout the surface 250 m (Fig. 3b). NH_4 concentrations were < 0.25 µmol l^{-1}, but reached concentrations of up to 0.4 µmol l^{-1} between 40–70 m depth (Table 1), while urea concentrations ranged from 1–1.5 µmol l^{-1} (Table 1). In the PFZ, surface NO_3 concentrations reached > 20 µmol l^{-1} (Fig. 3a), while $Si(OH)_4$ concentrations remained < 2 µmol l^{-1} in the upper 100 m of the water column (Fig. 3b). From north to south, surface NH_4 concentrations (above 100 m) gradually increased from < 0.25 to > 1.0 µmol l^{-1} (Table 1). Urea concentrations were higher than in the STZ and ranged from ~ 1 µmol l^{-1} to a maximum of 3.27 µmol l^{-1} (at ~ 60 m, station S3). Universally high nutrient concentrations were observed in the AZ. NO_3 concentrations exceeded 30 µmol l^{-1} in the surface ~ 100 m and continued to increase to a maximum of ~ 40 µmol l^{-1} with depth (Fig. 3a). $Si(OH)_4$ concentrations showed a steep north-south gradient from < 2 µmol l^{-1} north of the APF to > 60 µmol l^{-1} at the southern margin of the region (Fig. 3b). NH_4 and Urea concentrations in the AZ reached 0.8 and 2 µmol l^{-1} in the euphotic layer.

3.3 Chlorophyll-*a*

In the STZ, euphotic zone chl-*a* concentrations were highest, exceeding 0.4 µg l^{-1} with a sub-surface chl-*a* maximum (> 0.5 µg l^{-1}) at 30–40 m (Fig. 3c). A similar sub-surface maximum was observed for phaeopigments, although slightly deeper in the water column at 40–60 m (Fig. 3d). Size-fractionated chl-*a* showed that picophytoplankton contributed 50.4 % to total chl-*a* (Fig. 4b). In the SAZ, chl-*a* concentrations in the surface ~ 40 m exceeded 0.4 µg l^{-1} (Fig. 3c), whereas a sub-surface maximum in phaeopigments (> 0.3 µg l^{-1}) was observed at ~ 50 m (Fig. 3d). Size-fractionated chl-*a* indicated that nano- and picophytoplankton contributed 60.2 % and 39.8 %, respectively to total chl-*a* concentrations, while no microplankton were measured (Fig. 4) in the SAZ. In the PFZ, chl-*a* concentrations of ~ 0.3 µg l^{-1} were found in the upper 70 m, (Fig. 3c). Phaeopigments typically exceeded 0.1 µg l^{-1} in the upper 50 m of the water column,

BGD
8, 4917–4952, 2011

and remained $< 0.1\,\mu g\,l^{-1}$ below this depth (Fig. 3d). Size-fractionated chl-*a* in surface samples was dominated by nanophytoplankton (54.3 %) throughout this region (Fig. 4), followed by picophytoplankton (30.6 %) and microphytoplankton (15 %). Chl-*a* concentrations in the AZ between the PF and the SAccF, as well as south of the SBdy, ranged from 0.2 to $0.3\,\mu g\,l^{-1}$, while a band of low chl-*a* ($< 0.2\,\mu g\,l^{-1}$) was evident between the SAccF and the SBdy (Fig. 3c). Phaeopigments appeared completely absent in this region (Fig. 3d). In the AZ, nanoplankton comprised 61.9 % of the phytoplankton community, while micro and nano comprised 18.9 and 19.2 %, respectively (Fig. 4).

3.4 POC and PON

Maximum concentrations of POC ($14.1\,\mu mol\,l^{-1}$) and PON ($1.9\,\mu mol\,l^{-1}$) were found in the STZ just north of the STF (Fig. 3e, f) and confined to the upper 25 m. Average PON concentrations over the euphotic layer of the STZ were $1.02 \pm 0.57\,\mu mol\,l^{-1}$, with a mean euphotic zone C : N ratio of 7.16 ± 2.29. In the SAZ, POC and PON concentrations in the surface 40 m reached a maximum of 7.7 and $1.5\,\mu mol\,l^{-1}$, respectively (Fig. 3e, f), with a mean euphotic zone C : N ratio of $6.0 \pm 0.7\,\mu mol\,l^{-1}$. In the PFZ, POC and PON averaged $5.32 \pm 0.54\,\mu mol\,l^{-1}$ and $0.66 \pm 0.15\,\mu mol\,l^{-1}$, respectively in the upper 60 m of the water column (Fig. 3e, f), with both decreasing below this depth. The average C : N ratio in the euphotic zone was 8.2 ± 1.7. In the AZ, POC and PON were typically $< 4\,\mu mol\,l^{-1}$ and $< 0.5\,\mu mol\,l^{-1}$, respectively (Fig. 3e, f) in the euphotic zone, with a mean C : N ratio of 7.36 ± 2.66.

3.5 Nitrogen uptake

In the STZ ($n = 3$), ρurea dominated $\int \rho N$ by ~ 80 % (Fig. 5), reaching a maximum rate of $347\,nmol\,l^{-1}\,d^{-1}$ at 40 m at station S1 (Table 1). ρurea was on average 8 times greater than ρNO_3 or ρNH_4 yielding a mean f-ratio of 0.24 ± 0.22 (Table 2). Specific uptake of urea (V_{urea}) was on average 10 times greater than that of nitrate (V_{NO_3}) or ammonium (V_{NH_4}) (Fig. 6). In the SAZ ($n = 1$) ρNO_3 and ρurea reached

BGD
8, 4917–4952, 2011

maximum rates at 5 m of 157.3 and 197.2 nmol l^{-1} d^{-1}, respectively (Table 1). These values decreased to 54.7 and 46.4 nmol l^{-1} d^{-1}, respectively at the 1 % euphotic depth. $\int\rho$N was 10.3 mmol m^{-2} d^{-1}, with the highest contribution from $\int\rho NO_3$ (49.4 %) followed closely by $\int\rho$urea (43 %) (Fig. 5). The depth-integrated f-ratio for this station was 0.47 (Table 2). Specific uptake rates of nitrate (V_{NO_3}) and urea (V_{urea}) over the euphotic zone were 0.12 ± 0.05 d^{-1} and 0.13 ± 0.08 d^{-1} (Fig. 6), while V_{NH_4} was lower (0.02 ± 0.02 d^{-1}). In the PFZ ($n = 5$), euphotic zone ρNO_3, ρ urea and ρNH_4 remained below 50 nmol l^{-1} d^{-1} (Table 1) and were typically lower than uptake rates in the STZ and SAZ. Station S3 exhibited the highest ρN rates, compared to adjacent stations to the north or south. At station S3, ρNO_3 decreased from 124.0 nmol l^{-1} d^{-1} in the surface to 22.2 nmol l^{-1} d^{-1} at the base of the euphotic zone (Table 1). Conversely, ρ urea increased from 13.0 nmol l^{-1} d^{-1} in the surface to 108.5 nmol l^{-1} d^{-1} at depth. Average $\int\rho$N for the PFZ was 5.26 ± 2.2 mmol m^{-2} d^{-1} (Table 2), with the majority being due to $\int\rho NO_3$ (1.97 ± 0.46 mmol m^{-2} d^{-1}) and $\rho\int$urea (2.13 ± 1.78 mmol m^{-2} d^{-1}), while $\int\rho NH_4$ averaged 1.16 ± 0.41 mmol m^{-2} d^{-1}, resulting in a mean f-ratio of 0.41 ± 0.11 (Table 2). Average euphotic zone V_{NO_3}, V_{NH_4} and V_{urea} were 0.07 ± 0.07, 0.03 ± 0.1 and 0.04 ± 0.03 d^{-1}, respectively (Fig. 6). In the AZ ($n = 3$), ρNO_3, ρNH_4 and ρ urea also remained below 50 nmol l^{-1} d^{-1} (Table 1). Mean $\int\rho$N for the AZ was 6.46 ± 4.21 mmol m^{-2} d^{-1} (Table 1), with up to 50 % being derived from $\int\rho NO_3$ (3.43 ± 2.68 mmol m^{-2} d^{-1}) (Fig. 5, Table 2). Mean f-ratio in the AZ was 0.45 ± 0.11 (Table 2). Specific nitrogen uptake rates in the AZ were similar to those observed in the PFZ (Fig. 6).

4 Discussion

In this section we discuss nitrogen uptake dynamics across four different hydrographic regions in the Atlantic sector of the Southern Ocean. We highlight regional differences

BGD
8, 4917–4952, 2011

in uptake rates, f-ratios and community size structure and investigate how these change in relation to MLD, temperature, nutrients and surface dissolved iron concentrations. We compare our data with other ^{15}N estimates of production in the Southern Ocean, as well as with ^{234}Th based estimates of carbon export measured during the BGH cruise.

4.1 Regional comparisons of nitrogen uptake

4.1.1 The Subtropical Zone

Relatively high $\int\rho$N in the STZ (8.18 ± 6.8 mmol N m^{-2} d^{-1}) was dominated by $\int\rho$urea (~79 %), indicating significant regenerated production, as reflected by low f-ratios (0.24 ± 0.22). Similarly, V_{urea} was ten times higher than V_{NO_3} or V_{NH_4}. Low new production rates in this region are likely due to limiting surface NO_3 concentrations (< 0.05 µmol l^{-1}). Phytoplankton community structure was consistent with a typically regenerated-based community (Tremblay et al., 2000) with picophytoplankton dominating by ~ 51 % (Fig. 4). Similar low f-ratios ($f = 0.07 \pm 0.03$) were observed in the STZ of the Indian Sector (Table 2) (Thomalla et al., 2011). These results imply that this region of the Southern Ocean is dominated by urea re-cycling within the microbial loop, with little carbon export, little atmospheric CO_2 "draw-down", and conservation of nitrogen in surface waters (LeFevre et al., 1998; Smetacek et al., 2004).

4.1.2 The Subantarctic Zone

Station S2 in the SAZ exhibited only slightly higher total $\int\rho$N rates compared to those observed in the STZ, however this station showed a greater contribution of $\int\rho NO_3$ (49.4 %) (Fig. 5), which increased the f-ratio from 0.24 to 0.49 (Table 2). The highest V_{NO_3} of the cruise were also found at this station (0.12 d^{-1}) (Fig. 5) along with the highest concentrations of chl-a (> 0.5 µg l^{-1}), POC (> 7 µmol l^{-1}) and PON (> 1 µmol l^{-1}) (Fig. 3c, e, f), suggesting that there was some alleviation of iron stress (Lucas et al.,

BGD
8, 4917–4952, 2011

2007). It has been shown for oligotrophic regions that new production is enhanced within mesoscale eddy activity through the vertical injection of nutrients into the euphotic layer (Strass et al., 2002; Greenwood, 2007; Levy et. al., 2009). This station was on the edge of a mesoscale hydrographic feature, "anticyclone M" (Speich et al., 2011), observed just north of the SAF (Fig. 2). The proposed mechanism for the enhanced production and higher f-ratios at this station is enhanced vertical nutrient injection (including iron) at the edges of the anticyclone (Levy et al., 2009) along with an improved light environment associated with persistent shallow and stable mixed layers associated with the warm core eddy (Llido et al., 2005). Compared to observations in the SAZ of other sectors (Table 2), $\int\rho$N rates in this study were double $\int\rho$N rates in the Australian sector (Savoye et al., 2004), and less than half $\int\rho$N rates in the Indian sector (Thomalla et al., 2011). These differences are ascribed to differences in timing of the various cruises (spring, late summer, end of summer, Table 2). The high $\int\rho$N rates in the Indian sector were also due to high productivity downstream of the Subantarctic Islands, which was not present in the BGH transect.

4.1.3 The Polar Front Zone

Total $\int\rho$N rates in the PFZ were the lowest of the four regions (Table 1), with f-ratios of 0.41 ± 0.11. $\int\rho$urea and V_{urea} were substantially lower than the STZ and SAZ to the north (Figs. 5 and 6). Our $\int\rho$N rates in the PFZ were very similar to published $\int\rho$N rates for other PFZ sectors (Table 2), and also up to 80 % lower than during bloom conditions around Crozet (Lucas et al., 2007). Considering the timing of our cruise (late austral summer) and the relatively shallow mixed layers (68.7 ± 18.9 m) compared to the 1 % light depths (62 ± 11 m) it is unlikely that inadequate light limited primary production in this region. Surface Fe concentrations in this region were < 0.2 nmol l^{-1} (Chever et al., 2010). It is likely that the low uptake rates of this region are characteristic of the late summer season when phytoplankton growth is typically Fe-limited despite sufficient irradiance (Boyd et al., 2001; Lucas et al., 2007). Size-fractionated chlorophyll concentrations showed the PFZ to be dominated by nanophytoplankton (55 %, Fig. 4b).

BGD
8, 4917–4952, 2011

Several authors have found an increase in diatom concentration to be associated with the APF and attribute this to an increase in $Si(OH)_4$ (Laubscher et al., 1993; Bathmann et al., 1996, Smetacek et al., 1997; Tremblay et al., 2002). Although it is possible for diatoms to fall within the nanophytoplankton size range, substantial increases in $Si(OH)_4$ were only found south of the SAccF (Fig. 3b) and it is thus unlikely that the PFZ was associated with any increase in diatoms.

4.1.4 The Antarctic Zone

A slight increase in $\int \rho N$ was observed in the AZ ($7.5\,mmol\,m^{-2}\,d^{-1}$) relative to the PFZ ($5.3\,mmol\,m^{-2}\,d^{-1}$) with a simultaneous increase in f-ratios from 0.41 ± 0.11 to 0.45 ± 0.11 indicating a slightly higher potential for export. $\int \rho N$ from this study was in a similar range to the $\int \rho N$ of the permanently open AZ in the Australian sector (Savoye et al., 2004). Although, as expected, these open ocean $\int \rho N$ rates are however up to 70 % lower than those observed during bloom conditions in the Bellinghausen Sea ($26.4\,mmol\,N\,m^{-2}\,d^{-1}$) (Table 2). Lower open ocean $\int \rho N$ rates can be ascribed to the lack of dissolved iron inputs from melting ice (Sedwick and DiTullio, 1997; Gao et al., 2003; Grotti et al., 2005) and a less favourable light environment through deep mixed layer depths (93.9 ± 14.7 m) compared to the more stratified regions of the MIZ (Smith and Nelson, 1986).

4.2 ^{15}N estimates and ^{234}Th export flux

Carbon export derived from ^{234}Th deficits at 100 m revealed a north-south gradient, with the highest export fluxes (up to $6\,mmol\,C\,m^{-2}\,d^{-1}$) found south of the APF (Fig. 7, taken from Planchon et al., 2011). Although the latitudinal trend in f-ratio estimates of carbon export were not as clear, with high export being associated with the eddy in the SAZ, there was a similar tendency for carbon export to increase with latitude (Fig. 7). New production estimates of carbon export were however 2–20 times greater in magnitude (Fig. 7) than ^{234}Th derived estimates. Reasons for this are numerous. Firstly, the

BGD
8, 4917–4952, 2011

two methods used to estimate carbon export are not intended to measure the same process. Although the rates are expected to be comparable in a steady state system or when averaged over large enough time and space scales, there is otherwise no a priori reason why the rates should be identical. Stable isotope incubations measure NO_3 uptake at a discrete site over 12–24 h in the euphotic layer (typically < 60 m), while ^{234}Th deficit derived estimates of carbon export (at 100 m) encompass large space scales and a time period of ~ 31 days. Furthermore, ^{234}Th estimates are derived from particles > 50 µm, while ^{15}N does not discriminate on a size basis. ^{234}Th may well ignore a significant export flux within the < 50 µm fraction. This is also complicated by the POC : ^{234}Th ratio derived at the 100 m horizon; much deeper than the potential export horizon for ^{15}N. Hence, ^{234}Th more than likely represents a considerable averaging of episodically higher (or lower) fluxes when compared to short-term ^{15}N incubations. Intermittent events may potentially have a disproportionately large impact on overall flux budgets (McGillicuddy et al., 1997). For example, under-sampling episodic events of higher associated production can have profound effects on estimates of the metabolic balance of the sea (Karl et al., 2003). Furthermore, phytoplankton productivity measurements in the surface ocean at discrete locations may not represent mesoscale averages. Furthermore, the ^{234}Th method estimates particulate flux only, based on a measured POC : ^{234}Th ratio at 100 m, while new production represents the potential export of both dissolved and particulate material. Despite these discrepancies in magnitude, both proxies of export show the lowest rates of carbon export in the STZ with a tendency to increase with latitude to reach maximum rates of export south of the PF.

5 Conclusions

This paper presents ^{15}N-labelled nitrogen uptake measurements in the Atlantic Southern Ocean in late austral summer, 2008. ρN in the oligotrophic STZ was dominated by ρurea, resulting in low f-ratios (0.2). Size fractionated chl-*a* data also indicated a regenerated production based community in the STZ. The greatest $\int \rho$N was observed in

BGD
8, 4917–4952, 2011

the SAZ and ascribed to enhanced nutrient and favourable light conditions in an anticyclonic eddy. Higher f-ratios were observed in the SAZ ($f = 0.49$), Polar Frontal Zone (PFZ, $f = 0.41$) and Antarctic zone (AZ, $f = 0.45$) relative to the STZ (0.2) and indicate a higher contribution of ρNO_3 relative to total ρN in the regions further south. The observed trends in nitrogen dynamics resulted from a combination of shallow mixed layers in the north (~ 40 m) which progressively deepened (~ 100 m) with increased latitude. Increasing trends in ambient water column nutrient and surface iron concentrations corresponded with higher ρfN rates. These measurements allows for comparison with other proxies of production and carbon export in the Atlantic Southern Ocean.

Acknowledgements. We thank the officers and the crew of the R/V *Marion Dufresne* for their invaluable assistance in completing the BGH survey. We acknowledge Frederic Planchon, Frank Dehairs and Anne-Julie Cavagna for providing the unpublished ^{234}Th data collected during the cruise. We also thank Marie Boye, Annick Masson, Audrey Guenneugues and Frederic LeMoigne for providing the macronutrient, chl-*a* and POC data. This work was funded through the Southern Ocean Carbon – Climate Observatory (SOCCO) programme and the CSIR Parliamentary Grant. S. J. Thomalla was supported through a SOCCO post doctoral fellowship funded by ACCESS and NRF/SANAP.

References

Arrigo, K. R.: Marine microorganisms and global nutrient cycles, Nature, 437, 349–355, doi:10.1038/nature04158, 2005.

Arrigo, K. R., Van Dijken, G. L., and Bushinsky, S.: Primary production in the Southern Ocean, 1997–2006, J. Geophys. Res., 113, C08004, doi:10.1029/2007JC004551, 2008.

Banse, K.: Low seasonality of low concentrations of surface chlorophyll in the Subantarctic water ring: underwater irradiance, iron and grazing, Prog. Oceanogr., 37, 241–291, 1996.

Bathmann, U. V., Scharek, R., Klaas, C., Dubischar, C. D., and Smetacek, V.: Spring development of phytoplankton biomass and composition in major water masses of the Atlantic sector of the Southern Ocean, Deep-Sea Res. Pt. II, 44 (1–2), 51–67, 1997.

Behrenfeld, M. J.: Abandoning Sverdrups's critical depth hypothesis on phytoplankton blooms, Ecology, 91 (4), 997–989, 2010.

BGD

8, 4917–4952, 2011

Bianchi, M., Feliatra, F., Treguer, P., Vincendeau, M.-A., and Morvan, J.: Nitrification rates, ammonium nitrate distribution in upper layers of the water column and in sediments of the Indian sector of the Southern Ocean, Deep-Sea Res. Pt. II, 44 (5), 1017–1032, 1996.

Blain, S., Treguer, P., Belviso, S., Bucciarelli, E., Denis, M., Desabre, S., Fiala, M., Jezequel, V. M., Lefevre, J., Mayzaud, P., Marty, J.-C., and Razouls, S: A biogeochemical study of the island mass effect in context of the iron hypothesis: Kerguelen Island, Southern Ocean, Deep-Sea Res. Pt. I, 48, 163–187, 2001

Blain, S., Queguiner, B., Armand, L., Belviso, S., Bombled, B., Bopp, L., Bowie, A., Brunet, C., Brussaard, C., Carlotti, F., Christaki, U., Corbiere, A., Durand, I., Ebersbach, F., Fuda, J., Garcia, N., Gerringa, L., Griffiths, B., Guigue, C., Guillerm, C., Jacquet, S., Jeandel, C., Laan, P., Lefevre,., D., Lo Monaco, C., Malits, A., Mosseri, J., Obernosterer, I., Park, Y., Picheral, M., Pondaven, P., Remenyi, T., Sandroni, V., Sarthou, G., Savoye, N., Scouarnec, L., Souhaut, M., Thuiller, D., Timmermans, K., Trull, T., Uitz, J., van Beek, P., Veldhuis, M., Vincent, D., Viollier, E., Vong, L., and Wagener, T.: Effect of natural iron fertilization on carbon sequestration in the Southern Ocean, Nature, 446, 1070–1074, 2007.

Bowie, A. R., Maldonado, M. T., Frew, R. D., Croot, P. L., Achterberg, E. P., Fauzi, R., Mantoura, C., Worsfold, P. J., Law, C. S., and Boyd, P. W.: The fate of added iron during a mesoscale iron fertilisation experiment in the Southern Ocean, Deep-Sea Res. Pt. II, 48, 2703–2743, 2001.

Boyd, P. W.: The role of iron in the biogeochemistry of the Southern Ocean and Equatorial Pacific: a comparison of in situ iron enrichments, Deep-Sea Res. Pt. II, 49, 1803–1821, 2002.

Boyd, P. W., Crossley, A. C., DiTullio, G. R., Griffiths, F. B., Hutchins, D. A., Queguiner, B., Sedwick, P. N., and Trull, T. N.: Control of phytoplankton growth by iron supply and irradiance in the Subantarctic Ocean: experimental results from the SAZ project, J. Geophys. Res., 106, C12, 31573–31583, 2001.

Boyd, P. W., Jickells, T., Law, C. S., Blain, S., Boyle, E. A., Buesseler, K. O., Coale, K. H., Cullen, J. J., de Baar, H. J. W., Follows, M., Harvey, M., Lancelot, C., Levasseur, M., Owens, N. P. J., Pollard, R., Rivkin, R. B., Sarmiento, J., Schoemann, V., Smetacek, V., Takeda, S., Tsuda, A., Tumer, S., and Watson, A. J.: Mesoscale iron enrichment experiments 1993–2005: synthesis and future directions, Science, 315, 612–617, doi:10.1126/science.1131669, 2007.

Brzezinski, M. A., Dickson, M. L., Nelson, D. M., and Sambrotto, R.: Ratios of Si, C and N

BGD
8, 4917–4952, 2011

uptake by microplankton in the Southern Ocean, Deep-Sea Res. Pt. II, 50, 619–633, 2003.
Bury, S. J., Owens, N. J. P., and Preston, T.: ^{13}C and ^{15}N uptake by phytoplankton in the marginal ice-zone of the Bellingshausen Sea, Deep-Sea Res. Pt. II, 42, 1225–1252, 1995.
Caldeira, K. and Duffy, P. B.: The role of the Southern Ocean in uptake and storage of anthropogenic carbon dioxide, Science, 297, 620–622, 2000.
Chever, F., Bucciarelli, E., Sarthou, G., Speich, S., Arhan, M., Penven, P., and Tagliabue, A.: Physical speciation of iron in the Atlantic sector of the Southern Ocean, along transect from subtropical domain to the Weddell Sea Gyre, J. Geophys. Res., 115, C10059, doi:10.1029/2009JC005880, 2010.
Chrisholm, S. W. and Morel, F. M. M. M.: What controls phytoplankton production in nutrient-rich areas of the open sea?, Limnol. Oceanogr., 36 (8), U1507–U1511, 1991.
Clark, D., Rees, A. P., and Joint, I. R.: Ammonium regeneration and nitrification rates in the oligotrophic Atlantic Ocean: implications for new production estimates, Limnol. Oceanogr., 53 (1), 52–62, 2008.
Coale, K. H., Johnson, K. S., Chavez, F. P., Buesseler, K. O., Barber, R. T., Brzezinski, M. A., Cochlan, W. P., Millero, F. J., Falkowski, P. G., Bauer, J. E., Wanninkhof, R. H., Kudela, R. M., Altabet, M. A., Hales, B. E., Takahashi, T., Landry, M. R., Bidigare, R. R., Wang, X., Chase, Z., Strutton, P. G., Friederich, G. E., Gorbunov, M. Y., Lance, V. P., Hilting, A. K., Hiscock, M. R., Demarest, M., Hiscock, W. T., Sullivan, K. F., Tanner, S. J., Gordon, R. M., Hunter, C. N., Elrod, V. A., Fitzwater, S. E., Jones, J. L., Tozzi, S., Koblizek, M., Roberts, A. E., Herndon, J., Brewster, J., Ladizinsky, N., Smith, G., Cooper, D., Timothy, D., Brown, S. L., Selph, K. E., Sheridan, C. C., Twining, B. S., and Johnson, Z. I.: Southern Ocean iron enrichment experiment: carbon cycling in high- and low-Si waters, Science, 304, 408–414, 2004.
Cochlan, W. P.: Nitrogen uptake in the Southern Ocean, in: Nitrogen in the Marine Environment, edited by: Capone, D. G., Bronk, D. A., Mulholland, M., and Carpenter, E., Elsevier Press, Amsterdam, 561–588, 2008.
Cochlan, W. P., Bronk, D. A., and Coale, K. H.: Trace metals and nitrogenous nutrition of Antarctic phytoplankton: experimental observations in the Ross Sea, Deep-Sea Res. Pt. II, 49, 3365–3390, 2002.
Comiso, J. C., McClain, C. R., Sullivan, C. W., Ryan, J. P., and Leonard, C. L.: Coastal Zone Color Scanner pigment concentration in the Southern Ocean and relationship to geophysical surface features, J. Geophys. Res., 98, 2419–2451, 1993.
Cullen, J. J.: On models of growth and photosynthesis in phytoplankton, Deep-Sea Res., 37(4),

BGD
8, 4917–4952, 2011

667–683, 1990.
de Baar, H. J. W., Boyd, P. W., Coale, K. H., Landry, M. R., Atsuhsi, T., Assmy, P., Bakker, D. C. E., Bozec, Y., Barber, R. T., Brzezinski, M. A., Buesseler, K. O., Boyé, M., Croot, P. L., Gervais, F., Gorbunov, M. Y., Harrison, P. J., Hiscock, W. T., Laan, P., Lancelot, C., Law, C., Levasseur, M., Marchetti, A., Millero, F. J., Nishioka, J., Nojiri, Y., van Oijen, T., Riebesell, U., Rijkenberg, M. J. A., Saito, H., Takeda, S., Timmermans, K. R., Veldhuis, M. J. W., Waite, A., and Wong, C. S.: Synthesis of iron fertilization experiments: from the Iron Age in the Age of Enlightenment, in: The Oceans in a High-CO_2 World, edited by: Orr, J. C., Pantoja, S., and Pörtner, H.-O., J. Geophys. Res.-Oceans (Special Issue), 110, 1–24, 2005.
Dortch, Q.: The interaction between ammonium and nitrate uptake in phytoplankton, Mar. Ecol.-Prog. Ser., 61, 183–201, 1990.
Dugdale, R. C. and Goering, J. J.: Uptake of new and regenerated forms of nitrogen in primary production, Limnol. Oceanogr., 12, 196–206, 1967.
Dugdale, R. C. and Wilkerson, F. P.: Low specific nitrate uptake rate – a common feature of high-nutrient, low-chlorophyll marine ecosystems, Limnol. Oceanogr., 36, 1678–1688, 1991.
Eppley, R. W. and Peterson, B. J.: Particulate organic matter flux and planktonic new production in the deep ocean, Nature, 282, 677–680, 1979.
Froneman, P. W., Perissinotto, R., and McQuaid, C. D.: Seasonal variation in microzooplankton grazing in the region of the Subtropical Convergence, Mar. Biol., 126, 433–442, 1996.
Gao, Y., Fan, S., and Sarmiento, J. L.: Aeolian iron input to the ocean through precipitation scavenging: a modeling perspective and its implication for natural iron fertilization in the ocean, J. Geophys. Res., 108, 1–13, doi:10.1029/2002JD002420, 2003.
Gervais, F., Reibesell, U., and Gorbunof, M. Y.: Changes in primary productivity and chlorophyll a in response to iron fertilization in the Southern Polar Front Zone, Limnol. Oceanogr., 47(5), 1324–1335, 2002.
Grotti, M., Francesco, S., Carmela, I., and Roberto, F.: Trace metals distributions in coastal sea ice of Terra Nova Bay, Ross Sea, Antarctica, Antarct. Sci., 17, 290–300, 2005.
Glibert, P. M. and Garside, C.: Diel variability in nitrogenous nutrient uptake by phytoplankton in the Chesapeake Bay plume, J. Plankton Res., 14, 271–288, 1992.
Goeyens, L., Semeneh, M., Baumann, E. M., Elskens, M., Shopova, D., and Dehairs, F.: Phytoplankton nutrient utilization and nutrient signature in the Southern Ocean, J. Marine Syst., 17, 143–157, 1998.

BGD
8, 4917–4952, 2011

Greenwood, J. E., Feng, M., and Waite, A. M.: A one-dimensional simulation of biological production in two contrasting mesoscale eddies in the South Eastern Indian Ocean, Deep-Sea Res. Pt. II, 54, 1029–1044, 2007.
Korb, R. E. and Whitehouse, M.: Contrasting primary production regimes around South Georgia: large bloom vs. high nutrient low chlorophyll waters, Deep-Sea Res. Pt. I, 51, 721–738, 2004.
Laubscher, R. K., Perissinotto, R., and McQuaid, C. D.: Phytoplankton production and biomass at frontal zones in the Atlantic sector of the Southern Ocean, Polar Biol., 13, 471–481, 1993.
LeFèvre, J., Legendre, L., and Rivkin, R. B.: Fluxes of biogenic carbon in the Southern Ocean: roles of large microphagous zooplankton, J. Marine Syst., 17, 325–345, 1998.
Levy, M., Klein, P., and Jelloul, M. B.: New production stimulated by high-frequency winds in a turbulent mesoscale eddy field, Geophys. Res. Lett., 36, L16603, doi:10.1029/2009GL039490, 2009
Leynaert, A., Bucciarelli, E., Claquin, P., Dugdale, R. C., Martin-Jézéquel, V., Pondaven, P., and Ragueneau, O.: Effect of iron deficiency on diatom cell size and silicic acid uptake kinetics, Limnol. Oceanogr., 49(4), 1134–1143, 2004.
Llido, J., Garcon, V., Lutjeharms, J. R. E., and Sudre, J.: Event-scale blooms drive enhanced primary productivity at the Subtropical Convergence, Geophys. Res. Lett., 32, L15611, doi:10.1029/2005GL022880, 2005.
Lucas, M. I., Seeyave, S., Sanders, S., Moore, M. C., Williamson, R., and Stinchcombe, M.: Nitrogen uptake response to a naturally Fe fertilised phytoplankton bloom during the 2004/2005 CROZEX study, Deep-Sea Res. Pt. II, 54, 2138–2173, 2007.
Martin, J.: Glacial-interglacial CO_2 change: the iron hypothesis, Paleoceanography, 5, 1–3, 1990.
McCarthy, J. J.: The kinetics of nutrient utilization, in: Physiological Basis of Phytoplankton Ecology, edited by: Platt, T., Can. B. Fish. Aquat. Sci., 210, 211–233, 1981.
McGillicudy, D. J., Robinson, A. R., Siegel, D. A., Jannasch, H. W., Johnson, R., Dickey, T. D., McNeil, J., Michaels, A. F., and Knap, A. H.: Influence of mesoscale eddies on new production in the Sargasso Sea, Nature, 394, 263–266, 1998.
Mengesha, S., Dehairs, F., Fiala, M., Elskens, M., and Goeyens, L.: Seasonal variation of phytoplankton community structure and nitrogen uptake regime in the Indian Sector of the Southern Ocean, Polar Biol., 20, 259–272, 1998.
Metzl, N., Tilbrook, B., and Poisson, A.: The annual fCO_2 cycle and the air-sea CO_2 flux in the

BGD
8, 4917–4952, 2011

sub-Antarctic Ocean, Tellus, 51B, 849–861, 1999.
Mitchell, B. G., Brody, E. A., Holm-Hansen, O., McClain, C., and Bishop, J.: Light limitation of phytoplankton biomass and macronutrient utilization in the Southern Ocean, Limnol. Oceanogr., 36(8), 1662–1677, 1991.
Moore, C. M., Hickman, A. E., Poulton, A. J., Seeyave, S., and Lucas, M. I.: Iron-light interactions during the CROZet natural iron bloom and EXport experiment (CROZEX): II – Taxonomic responses and elemental stoichiometry, Deep-Sea Res. Pt. II, 54, 2066–2084, 2007.
Moore, J. K. and Abbott, M. R.: Surface chlorophyll concentrations in relation to the Antarctic Polar Front: seasonal and spatial patterns from satellite observations, J. Marine Syst., 37, 69–86, 2002.
Nelson, D. M. and Smith, W. O.: Sverdrup revisited: critical depths, maximum chlorophyll levels, and the control of Southern Ocean productivity by the irradiance-mixing regime, Limnol. Oceanogr., 36(8) 1650–1661, 1991.
Planchon, F., Cavagna, A. J., and Dehairs, F.: Dynamics of biogenic particles in the Southern Atlantic Ocean as revealed by ^{234}Th proxy along the Bonus-Good-Hope transect from Cape Basin to Northern Weddell gyre, Biogeosciences Discuss., in preparation, 2011.
Pollard, R. T., Lucas, M. I., and Read, J. F.: Physical controls on biogeochemical zonation in the Southern Ocean, Deep-Sea Res. Pt. II, 49, 3289–3305, 2002.
Pollard, R. T., Venables, H. J., Read, J. F., and Allen, J. T.: Large scale circulation around the Crozet Plateau controls an annual phytoplankton bloom in the Crozet Basin, Deep-Sea Res. Pt. II, 54, 1915–1929, 2007.
Pollard, R. T., Salter, I., Sanders, R. J., Lucas, M. I., Moore, C. M., Mills, R. A., Statham, P. J., Allen, J. T., Baker, A. R., Bakker, D. C. E., Charette, M. A., Fielding, S., Fones, G. R., French, M., Hickman, A. E., Holland, R. J., Hughes, J. A., Jickells, T. D., Lampitt, R. S., Morris, P. J., Nedelec, F. H., Nielsdottir, M., Planquette, H., Popova, E. E., Poulton, A. J., Read, J. F., Seeyave, S., Smith, T., Stinchcombe, M., Taylor, S., Thomalla, S., J., Venables, H. J., Williamson, R., and Zubkov, M. V.: Southern Ocean deep-water carbon export enhanced by natural iron fertilization, Nature, 457, 577–580, 2009.
Price, N. M., Ahner, B. A., and Morel, F. M. M.: The Equatorial Pacific Ocean: Grazer-controlled phytoplankton in an iron-limited ecosystem, Limnol. Oceanogr., 39(3), 520–534, 1994.
Priddle, J., Boyd, I. L., Whitehouse, M. J., Murphey, E. J., and Croxall, J. P.: Estimates of Southern Ocean primary production – constraints from predator carbon demand and nutrient

BGD
8, 4917–4952, 2011

drawdown, J. Marine Syst., 17, 275–288, 1998.
Probyn, T. A., Waldron, H. N., Searson, S., and Owens, N. J. P.: Diel variability in nitrogenous nutrient uptake at photic and subphotic depths, J. Plankton Res., 18, 2063–2079, 1996.
Raven, J. A.: The iron and molybdenum use efficiencies of plant growth with different energy, carbon and nitrogen sources, New Phytol., 109, 279–288, 1988.
Raven, J. A.: Predictions of Mn and Fe use efficiencies of phototrophic growth as a function of light availability for growth and of C assimilation pathway, New Phytol., 116, 1–18, 1990.
Savoye, N., Dehairs, F., Elskens, M., Cardinal, D., Kopczynska, E. E., Trull, T. W., Wright, S., Baeyens, W., and Griffiths, F. B.: Regional variation of spring N-uptake and new production in the Southern Ocean, Geophys. Res. Lett., 31, L03301, doi:10.1029/2003GL018946, 2004.
Sambrotto, R. N. and Mace, B. J.: Coupling of biological and physical regimes across the Antarctic Polar Front as reflected by nitrogen production and recycling, Deep-Sea Res. Pt. II, 47, 3339–3367, 2000.
Sedwick, P. N. and DiTullio, G. R.: Regulation of algal blooms in Antarctic shelfwater by the release of iron from melting sea ice, Geophys. Res. Lett., 24, 2515–2518, 1997.
Sedwick, P. N., Blain, S., Queguiner, B., Griffiths, F. B., Fialla, M., Bucciarelli, E., and Denis, M.: Resource limitation of phytoplankton growth in the Crozet Basin, Subantarctic Southern Ocean, Deep-Sea Res. Pt. II, 49, 3327–3349, 2002.
Seeyave, S., Lucas, M., Moore, C. M., and Poulton, A. J.: Phytoplankton productivity and community structure in the vicinity of Crozet Plateau during austral summer 2004/2005, Deep-Sea Res. Pt. II, 54, 2020–2044, 2007.
Sigman, D. M. and Boyle, E. A.: Glacial/Interglacial variations in atmospheric carbon dioxide, Nature, 407, 859–869, 2000.
Smetacek, V., de Baar, H. J. W., Bathmann, U. V., Lochte, K., and Van Der Loeff, M. M. R.: Ecology and biogeochemistry of the Antarctic Circumpolar Current during austral spring: a summary of Southern Ocean JGOFS cruise ANT X/6 of, R. V. Polarstern, Deep-Sea Res. Pt. II, 44, 1–21, 1997.
Smetacek, V., Assmy, P., and Henjes, J.: The role of grazing in structuring Southern Ocean pelagic ecosystems and biogeochemical cycles, Antarct. Sci., 16(4), 541–558, 2004.
Smith Jr., W. O. and Nelson, D. M.: Importance of ice edge phytoplankton production in the Southern Ocean, BioScience, 36, 251–257, 1986.
Sokolov, S. and Rintoul, S. R.: On the relationship between fronts of the Antarctic Circumpolar Current and surface chlorophyll concentrations in the Southern Ocean, J. Geophys. Res.,

BGD
8, 4917–4952, 2011

112, C07030, doi:10.1029/2006JC004072, 2007.
Speich, S., Arhan, M., and Fine, R. A.: Water masses and ocean dynamics along the BONUS-GoodHope transect, Ocean Sci. Discuss., in preparation, 2011.
Strass, V. H., Garabato, A. C. N., Pollard, R. T., Fischer, H. I., Hense, I., Allen, J. T., Read, J. F., Leach, H., and Smetacek, V.: Mesoscale frontal dynamics: shaping the environment of primary production in the Antarctic Circumpolar Current, Deep-Sea Res. Pt. II, 49, 3735–3769, 2002.
Sullivan, C. W., Arrigo, K. R., McClain, C. R., Comiso, J. C., and Firestone, J.: Distributions of phytoplankton blooms in the Southern Ocean, Science, 262, 1832–1837, 1993.
Takahashi, T., Sutherland, S. C., Sweeny, C., Poisson, A., Metzl, N., Tilbrook, B., Bates, N., Wanninkof, R., Feely, R. A., Sabine, C., Olafsson, J., and Yukihiro, N.: Global sea-air CO_2 flux based on climatological surface ocean pCO_2, and seasonal biological temperature effects, Deep-Sea Res. Pt. II, 49, 1601–1622, 2002.
Thomalla, S. J., Waldron, H. N., Lucas, M. I., Read, J. F., Ansorge, I. J., and Pakhomov, E.: Phytoplankton distribution and nitrogen dynamics in the southwest indian subtropical gyre and Southern Ocean waters, Ocean Sci., 7, 113–127, doi:10.5194/os-7-113-2011, 2011.
Thompson, P. A., Levasseur, M. E., and Harrison, P. J.: Light limited growth on ammonium vs. nitrate: what is the advantage for marine phytoplankton?, Limnol. Oceanogr., 34, 1014–1024, 1989.
Treguer, P. and Jacques, G.: Dynamics of nutrients and phytoplankton, and fluxes of carbon, nitrogen and silicon in the Antarctic Ocean, Polar Biol., 12, 149–162, 1992.
Tremblay, J. E., Legendre, L., Klein, B., and Therriault, J. C.: Size-differential uptake of nitrogen and carbon in a marginal sea (Gulf of St. Lawrence, Canada): significance of diel periodicity and urea uptake, Deep-Sea Res. Pt. II, 47, 489–518, 2000.
Tremblay, J. E., Lucas, M. I., Kattner, G., Pollard, R., Strass, V. H., Bathmann, U., and Bracher, A.: Significance of the Polar Front Zone for large-sized diatoms and new production during summer in the Atlantic sector of the Southern Ocean, Deep-Sea Res. Pt. II, 49, 3793–3811, 2002.
Trull, T. W., Davies, D., and Casciotti, K.: Insights into nutrient assimilation and export in naturally iron fertilized waters of the Soutern Ocean from nitrogen, carbon and oxygen isotopes, Deep-Sea Res. Pt. II, 55, 820–840, 2008.
Venables, H. and Moore, C. M.: Phytoplankton and light limitation in the Southern Ocean: learning from high nutrient, high chlorophyll areas, J. Geophys. Res., 115, C02015,

BGD
8, 4917–4952, 2011

doi:10.1029/2009JC005361, 2010.
Waldron, H. N., Attwood, C. G., Probyn, T. A., and Lucas, M. L.: Nitrogen dynamics in the Bellinghausen Sea during the austral spring of 1992, Deep-Sea Res. Pt. II, 42(4–5), 1253–1276, 1995.
Whitehouse, M. J., Korb, R. E., Atkinson, A., Thorpe, S. E., and Gordon, M.: Formation, transport and decay of an intense phytoplankton bloom within the high-nutrient low Chlorophyll belt of the Southern Ocean, J. Marine Syst., 70, 150–167, 2008.
Yool, A., Martin, A. P., Fernandez, C., and Clark, D. R.: The significance of nitrification for oceanic new production, Nature, 447, 999–1002, doi:10.1038/nature05885, 2007.

BGD
8, 4917–4952, 2011

Table 1. List of data for at each sampling station during the BGH cruise (chl-*a*, $\mu g\,l^{-1}$; POC and PON, $\mu mol\,l^{-1}$; nutrients, $\mu mol\,l^{-1}$; ρN, $nmol\,l^{-1}\,d^{-1}$).

Station	Depth	Chl-*a*	POC	PON	NO_3	NH_4	Urea	ρNO_3	ρNH_4	ρ urea	*f*
STZ											
L1	1.0	0.05	5.36	0.94	0.25	0.06	0.22	14.4	12.7	10.7	0.38
	5.0	0.05	8.13	0.68	0.25	0.05	0.33	9.5	26.0	30.5	0.14
	9.1	0.06	1.80	0.25	0.25	0.01	0.11	13.9	29.0	20.0	0.22
	35.0	0.11	4.78	0.82	0.25	0.02	0.33	21.2	34.5	49.8	0.20
	80.9	0.47	3.36	0.46	3.24	0.01	0.33	4.9	2.7	61.7	0.07
S1	1.0	0.14	4.36	0.59	0.25	0.02	0.86	5.5	17.4	245.1	0.02
	7.3	0.16	4.50	0.62	0.25	0.01	0.76	20.1	18.4	280.2	0.06
	14.0	0.17	4.56	0.64	0.25	0.06	0.32	17.8	20.3	133.5	0.10
	40.2	0.20	5.42	0.71	0.25	0.10	0.86	18.2	16.3	347.5	0.05
	53.6	0.37	7.06	0.99	0.25	0.17	0.76	5.0	4.9	264.7	0.02
L2	1.0	0.49	12.26	1.93	2.01	0.08	1.51	1.4	32.0	330.5	0.00
	3.3	0.54	12.26	1.93	2.01	0.08	0.65	37.5	37.7	169.0	0.15
	7.8	0.55	12.27	1.77	2.50	0.10	1.08	53.2	42.8	294.2	0.14
	15.3	0.56	14.12	1.88	3.86	0.03	0.76	56.6	17.6	105.0	0.32
	35.4	0.40	6.07	0.90	3.99	0.51	0.65	7.0	5.9	41.6	0.13
											0.13
SAZ											
S2	1.0	0.35	7.70	1.30	11.04	0.09	1.26	41.0	15.9	50.0	0.38
	5.0	0.35	7.24	1.48	10.80	0.09	2.11	157.2	30.1	197.2	0.41
	9.6	0.35	7.68	1.15	10.80	0.09	0.84	96.7	21.8	57.6	0.55
	21.9	0.34	7.48	1.30	10.80	0.09	1.37	132.2	25.9	105.1	0.50
	50.6	0.38	5.78	0.89	6.03	0.09	1.26	54.7	1.8	46.7	0.53

BGD
8, 4917–4952, 2011

Table 1. Continued.

Station	Depth	Chl-*a*	POC	PON	NO_3	NH_4	Urea	ρNO_3	ρNH_4	ρ urea	*f*
PFZ											
L3	1.0	0.25	4.78	0.78	17.79	0.31	0.71	30.7	23.4	26.4	0.38
	10.0	0.25	4.57	0.64	nd	nd	1.29	nd	nd	50.7	nd
	20.2	0.25	4.78	0.68	nd	0.31	0.82	nd	25.8	34.0	nd
	40.0	0.26	4.65	0.78	nd	nd	0.59	nd	nd	35.6	nd
	60.9	0.25	4.57	0.64	17.67	0.31	nd	56.8	5.1	nd	0.92
L4	1.0	0.40	6.97	0.78	18.68	0.67	1.37	17.6	6.3	36.0	0.29
	10.6	0.40	6.67	0.80	18.68	0.67	0.91	33.1	22.0	18.2	0.45
	18.9	0.40	6.51	0.88	18.44	0.68	0.91	53.4	29.4	44.1	0.42
	20.3	0.40	5.63	0.75	18.44	0.68	1.03	45.6	35.7	15.3	0.47
	48.9	0.40	6.04	0.78	18.92	0.69	1.94	43.0	26.7	8.0	0.55
S3	1.0	0.36	6.04	0.86	21.12	0.60	0.24	124.0	39.6	13.0	0.70
	5.0	0.36	6.04	0.86	21.12	0.60	0.85	72.0	24.6	16.9	0.63
	9.5	0.36	5.89	0.88	20.88	0.60	0.85	40.2	21.0	14.0	0.53
	19.7	0.36	5.58	0.74	21.12	0.60	1.58	28.3	48.1	106.8	0.15
	60.1	0.36	5.56	0.80	20.88	0.62	3.27	22.2	8.4	108.5	0.16
L5	1.0	0.26	5.17	0.47	20.93	0.73	0.39	37.1	8.2	5.6	0.73
	3.9	0.26	5.17	0.47	20.93	0.73	0.39	20.6	9.3	3.0	0.63
	10.1	0.26	5.49	0.53	20.93	0.73	2.06	21.0	14.4	13.2	0.43
	13.9	0.28	5.19	0.47	20.93	0.73	1.42	39.1	18.8	15.3	0.53
	60.4	0.25	5.16	0.60	20.93	0.73	0.77	15.5	15.3	10.5	0.38
L6	1.0	0.31	5.37	0.54	22.80	1.26	nd	14.6	4.3	nd	0.77
	5.7	0.31	5.37	0.54	22.80	1.26	1.58	18.1	6.2	20.1	0.41
	9.4	0.30	9.04	0.74	22.80	1.25	1.33	22.9	7.4	28.3	0.39
	15.2	0.30	5.23	0.47	22.80	1.26	1.94	23.5	11.5	48.4	0.28
	78.5	0.30	3.43	0.31	24.51	1.89	1.33	13.6	5.5	13.3	0.42

BGD
8, 4917–4952, 2011

Table 1. Continued.

Station	Depth	Chl-*a*	POC	PON	NO_3	NH_4	Urea	ρNO_3	ρNH_4	ρ urea	*f*
AZ											
S4	1.00	0.16	2.67	0.50	nd	0.80	2.00	nd	11.0	24.7	nd
	1.90	0.16	2.67	0.50	25.71	0.80	2.00	28.8	11.6	16.9	0.50
	13.50	0.17	2.72	0.50	25.71	0.79	2.19	20.9	8.5	12.5	0.50
	23.60	0.16	2.98	0.50	25.71	0.80	1.62	19.7	9.2	16.8	0.43
	88.30	0.16	2.60	0.40	25.96	0.79	1.43	10.8	7.1	8.7	0.41
L7	1.0	0.25	5.37	0.54	28.08	0.46	0.83	28.0	14.4	11.0	0.52
	5.3	0.25	9.04	0.74	28.08	0.46	0.41	51.1	13.0	8.0	0.71
	13.5	0.24	5.23	0.47	28.08	0.43	1.33	42.3	15.0	19.4	0.55
	25.1	0.27	5.39	0.52	28.08	0.43	1.94	53.3	3.7	41.5	0.54
	109.9	0.28	2.05	0.19	29.76	0.31	1.33	45.4	14.3	18.4	0.58
S5	1.0	0.33	4.48	0.76	27.81	0.61	1.68	47.5	20.0	29.3	0.49
	3.2	0.33	4.48	0.76	27.81	0.61	1.29	41.2	23.8	29.3	0.44
	8.5	0.33	4.63	1.03	27.81	0.61	2.06	45.2	27.6	43.4	0.39
	28.8	0.30	4.06	0.69	28.06	0.63	3.10	33.3	19.5	73.0	0.26
	90.0	0.21	3.55	0.68	28.06	0.62	1.16	36.1	22.8	21.1	0.45

BGD
8, 4917–4952, 2011

Table 2. Comparison of depth integrated values of ^{15}N uptake (mmol m^{-2} d^{-1}) by phytoplankton in various regions of the Southern Ocean.

Region/Description	$\int \rho NO_3$	$\int \rho NH_4$	$\int \rho$urea	$\Sigma \int \rho N$	f-ratio	
Atlantic Sector (summer 2008, BGH)						this study
STZ (34-41° S)	1.01 ± 0.3	0.69 ± 0.3	6.47 ± 6.7	8.18 ± 6.8	0.24 ± 0.22	
SAZ (42–44° S)	5.11	0.92	4.31	10.34	0.49	
PFZ (45–50° S)	1.97 ± 0.5	1.16 ± 0.4	2.13 ± 1.8	5.26 ± 2.2	0.41 ± 0.11	
AZ (51–57° S)	3.39 ± 1.9	1.27 ± 0.6	2.86 ± 1.6	7.51 ± 3.5	0.45 ± 0.11	
Australian Sector (spring 2001, CLIVAR-SR3)						Savoye et al. (2004)
SAZ/STF (49–51.0° S)				4.4 ± 0.3	0.53 ± 0.26	
PFZ/IPFZ (54–57° S)				5.6 ± 0.1	0.56 ± 0.02	
AZ/MIZ (61–65° S)				9.6 ± 2.2	0.61 ± 0.08	
Bellinghausen Sea						Waldron et al. (1996)
Open Pacific (Stn 12234; 57° S)	2.6	13.65	10.13	26.38	0.09	
PFZ (Stn 12230; 64° S)	0.9	8.1	9.61	9.61	0.1	
Indian Sector (CROZEX, summer 2004)						Lucas et al. (2007)
Crozet-M3 bloom	20.3 ± 5.7	3.6 ± 1.3	6.1 ± 2.0	30.1 ± 7.5	0.67 ± 0.08	
Crozet-South of Plateau (HNLC)	1.8 ± 0.8	3.2 ± 0.5	1.1 ± 0.2	6.0 ± 1.5	0.28 ± 0.07	
Indian Sector (summer 1994, ANTARES3)						Mengesha et al. (1998)
Kerguelen Plateau (Stn A18; 49° S)	5.7	3.5	2.8	11.9	0.48	
Kerguelen Plateau (Stn A16; 52° S)	7.7	2	1	10.7	0.72	
Indian Sector (late summer 1999, MIOS-4)						Thomalla et al. (2011)
STZ (31–40° S)	3.76 ± 4.2	19.83 ± 15.0	22.30 ± 17.8	46.07 ± 33.5	0.07 ± 0.03	
SAZ (41–47° S)	2.90 ± 3.4	14.97 ± 16.9	6.86 ± 3.9	24.73 ± 21.6	0.10 ± 0.04	
Pacific Sector (summer 1997, US-JGOFS)						Sambrotto and Mace (2000)
PFZ (57–61° S)	2-5 ± 2.3				0.05–0.48	

BGD
8, 4917–4952, 2011

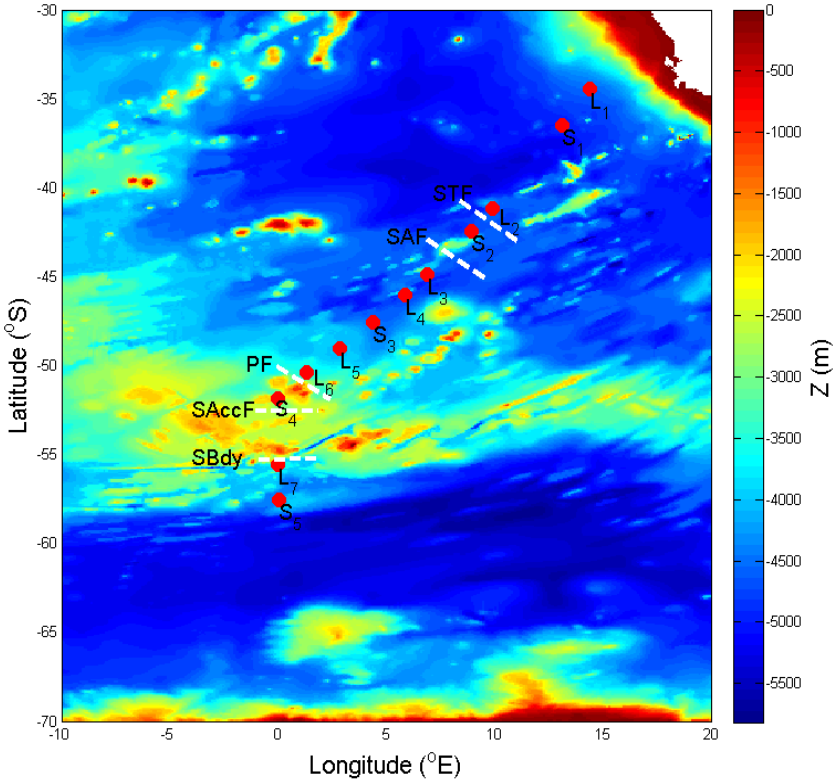

Fig. 1. Cruise track during the Bonus Goodhope 2008 campaign. Red dots indicate the sampling positions for ^{15}N uptake experiments. The hydrographic fronts, Subtropical Front (STF), Sub-Antarctic Front (SAF), Polar Front (PF), South Antarctic Circumpolar Current Front (SAccF) and Southern Boundary (Sbdy) are indicated by dotted white lines.

BGD
8, 4917–4952, 2011

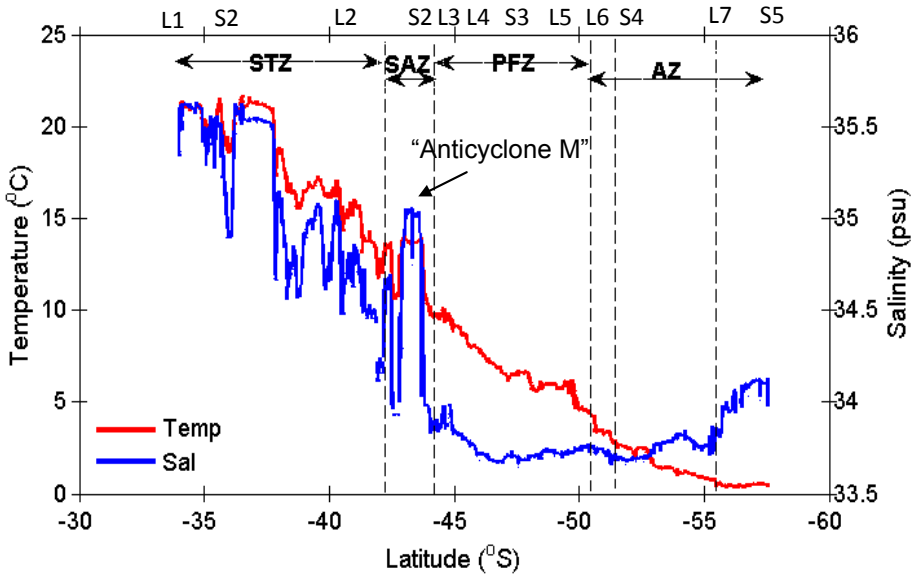

Fig. 2. Surface temperature (red line) and surface salinity (blue line) with latitude along the cruise track. Sampling station identifiers are indicated above the plot. It shows the zonal description of the regions during the cruise (Sub Tropical Zone (STZ), Sub Antarctic Zone (SAZ), Polar Front Zone (PFZ) and Antarctic Zone (AZ). The position of Anticyclone M is indicated by the increase in temperature and salinity in the SAZ.

BGD
8, 4917–4952, 2011

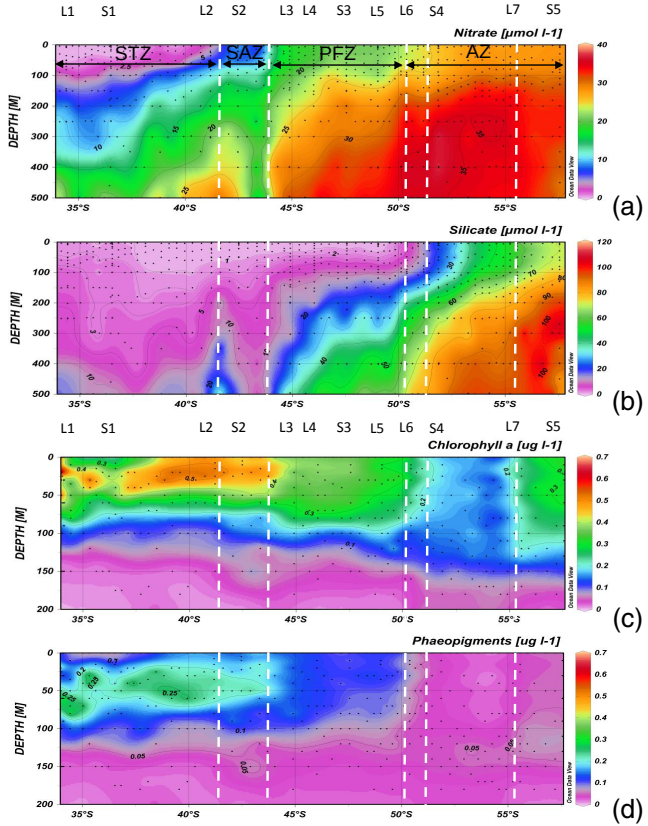

Fig. 3. (a, b, c, d) Profiles of NO_3, $Si(OH)_4$ in the upper 500 m and chl-*a*, phaeopigments, PON and POC in the upper 200 m of the water column along the Bonus-Goodhope cruise track. Productivity station positions are indicated on the top of each plot. Nutrient, chl-*a* and phaeopigment data courtesy of M. Boye (personal communication, 2008).

BGD
8, 4917–4952, 2011

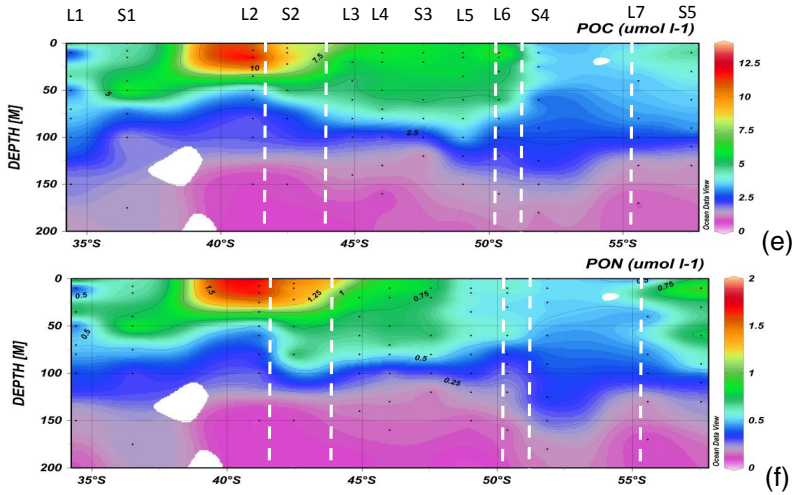

Fig. 3. (e, f) PON and POC in the upper 200 m of the water column. Productivity stations are indicated on the top of the plot. Data courtesy of M. Boye and A. Masson (personal communication, 2008).

BGD
8, 4917–4952, 2011

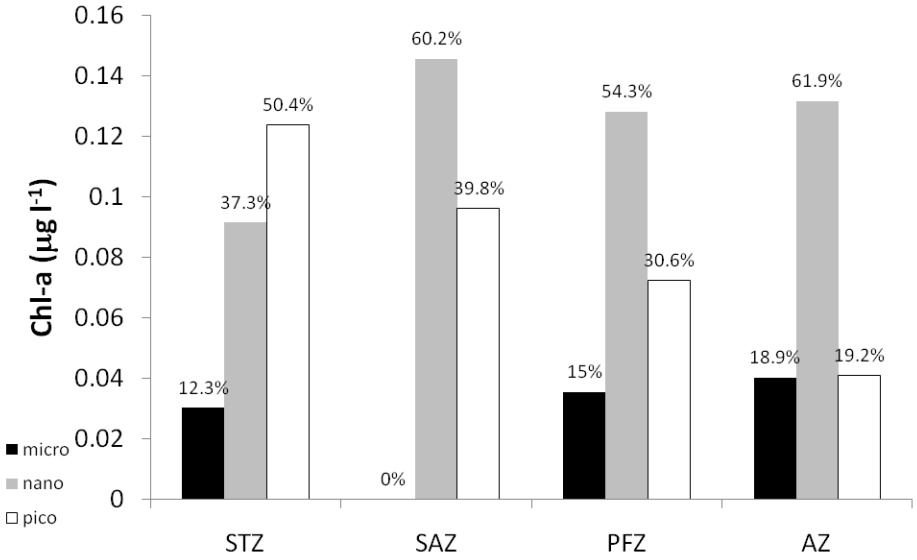

Fig. 4. Size fractionated chl-*a* of surface samples in each region along the BGH cruise track. Percentage of the total is presented at the top of each bar. It shows the decreasing contribution of picophytoplankton from north to south along the cruise track.

BGD
8, 4917–4952, 2011

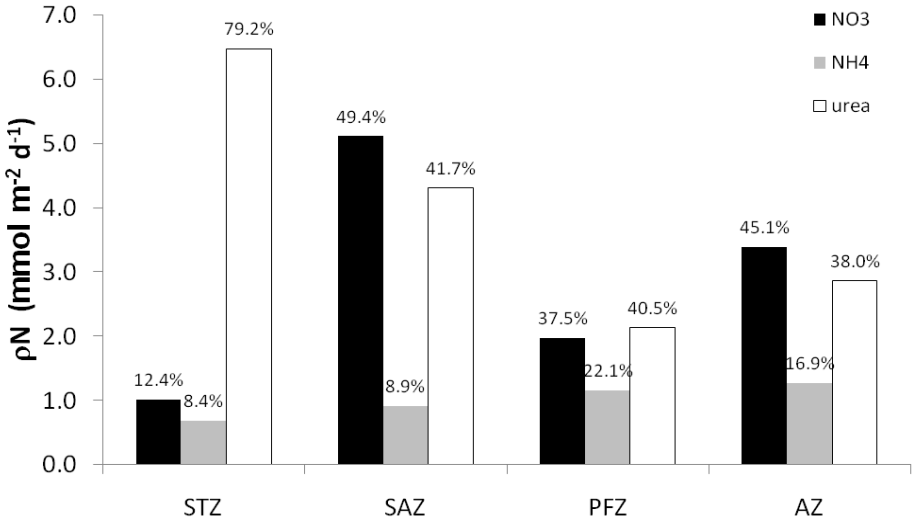

Fig. 5. Depth integrated nitrogen uptake ($\int \rho N$) in each zonal region. It shows the contribution $\int \rho NO_3$ (black), $\int \rho NH_4$ (grey) and $\int \rho$urea (white) as % of total uptake.

BGD
8, 4917–4952, 2011

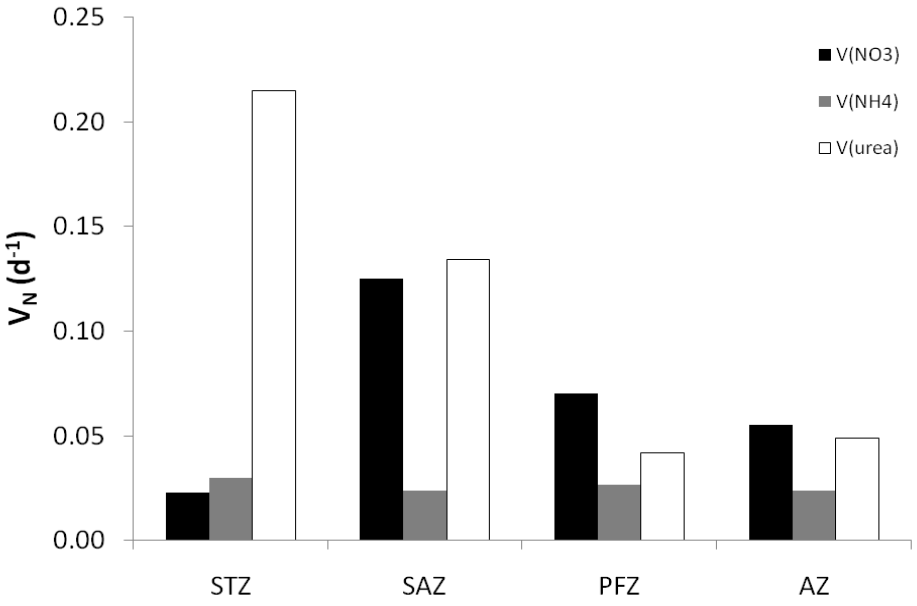

Fig. 6. Specific uptake (V, h^{-1}) averaged over the euphotic zone for each region. It shows the contribution V_{NO_3} (black), V_{NH_4} (grey) and V_{urea} (white) as % of total uptake, and a decreasing trend V_{urea} from north to south.

BGD
8, 4917–4952, 2011

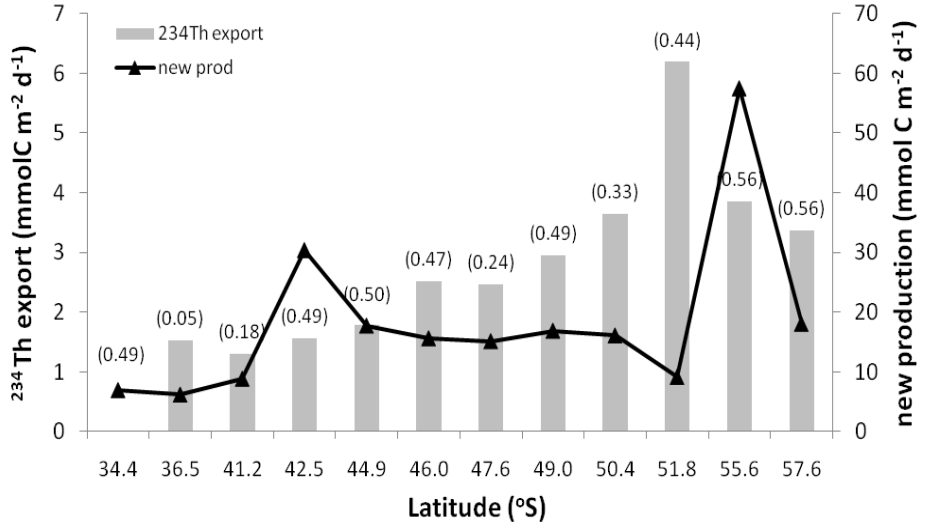

Fig. 7. Comparison between ^{234}Th export (at 100 m) (grey bars) and "new production" estimates (black triangles) during BGH. New production calculated from $\int \rho NO_3$ and the C : N ratio. It shows the difference in magnitude of these proxies of carbon export. ^{234}Th data from Planchon et al. (2011).

BGD
8, 4917–4952, 2011